Measurements of target compressive and tensile strength for application to impact cratering on ice-silicate mixtures

Hiraoka, Kensuke
Arakawa, Masahiko
Setoh, Masato
Nakamura, Akiko M.

JOURNAL OF GEOPHYSICAL RESEARCH, VOL. 113, E02013, doi:10.1029/2007JE002926, 2008

Measurements of target compressive and tensile strength for application to impact cratering on ice-silicate mixtures

Kensuke Hiraoka,[1] Masahiko Arakawa,[2] Masato Setoh,[1] and Akiko M. Nakamura[1]

Received 13 April 2007; revised 9 October 2007; accepted 2 November 2007; published 28 February 2008.

[1] Small icy bodies in the outer solar system have been shown to consist of ice-silicate mixtures. The results of previous impact cratering experiments on ice-silicate mixture targets showed that a crater volume decreases with increasing silicate content. Surface strength controls craterings in laboratory experiments and on small bodies with a certain degree of strength. In this study we measured the uniaxial compressive and tensile strength of the targets used in previous impact cratering experiments by uniaxial compression and Brazilian tests, respectively, at 263 K and calculated the shear strength from the measured values. We found the uniaxial compressive and tensile strength increased with silicate content, which explains why the crater volume decreases with increasing silicate content. Since the gradient of increase of the uniaxial compressive and the tensile strength was different, the difference between the tensile strength and the uniaxial compressive strength becomes smaller with the increase of silicate content up to 50 wt %. We show that the crater spall diameter is better scaled by the tensile strength to compensate the difference of the silicate content than by the uniaxial compressive strength.

Citation: Hiraoka, K., M. Arakawa, M. Setoh, and A. M. Nakamura (2008), Measurements of target compressive and tensile strength for application to impact cratering on ice-silicate mixtures, *J. Geophys. Res.*, *113*, E02013, doi:10.1029/2007JE002926.

1. Introduction

[2] Pure ice has been often used in laboratory impact experiments in order to simulate the impact process on icy bodies [e.g., *Kato et al.*, 1995]. From data of spacecrafts, however, it has been shown that comets, Saturn's rings and satellites in the outer solar system consist of several kinds of volatiles (N_2, CO_2, CH_4 and H_2O) and silicate dusts [e.g., *Keller et al.*, 2005; *Estrada and Cuzzi*, 1996; *Kempf et al.*, 2005; *Porco et al.*, 2005]. When these small bodies have a certain degree of strength, crater formation is controlled by the strength, defining what is called the "strength regime" [*Holsapple*, 1993]. In this strength regime, the mechanical strength of the material is a key parameter to determine the crater dimension and morphology. In fact, images taken by the Stardust mission show pit halo depressions like Rahe crater and flat floor craters on the surface of Comet 81 P/Wild 2, and similar structures were observed in laboratory hypervelocity impact experiments by using strength controlled targets [*Brownlee et al.*, 2004]. They used baked resin-coated sand for the analogue of comet nucleus. Although they succeeded to reproduce the characteristic crater morphologies observed, the experimental condition obtained was unrealistic for the crater made on the comet, because the baked resin-coated sand could have a very different mechanical strength from the comet nucleus. Ice-silicate mixtures are the main components to construct the small icy bodies. Thus we should study the mechanical strength of not only pure ice but also ice-silicate mixtures in order to understand the impact cratering on the small icy bodies.

[3] Previous impact cratering experiments on ice-silicate mixtures showed that a crater size decreases with increasing silicate content [*Lange and Ahrens*, 1982; *Koschny and Grün*, 2001; *Hiraoka et al.*, 2007]. *Koschny and Grün* [2001] conducted impact cratering experiments on ice-silicate mixtures at about 1 to 10 km s^{-1}. They found the crater volume decreased with increasing silicate content [see *Koschny and Grün*, 2001, Figure 9]; however, the silicate content was quite limited below 20 wt %. This negative tendency of the crater volume to the silicate content was found to extend up to silicate content of 50 wt % by *Hiraoka et al.* [2007].

[4] The mechanical strength of ice-silicate mixtures, which controls the cratering processes, depends not only on silicate content but also target porosity. *Arakawa and Tomizuka* [2004] found that the static compressive strength of sintered ice-silicate mixtures at a strain rate of 5.6×10^{-3} s^{-1} followed an empirical power law equation of the porosity from 12.5 to 37%, and the strength was always lower than that of sintered pure ice. They examined the samples with the silicate content of 50 wt % only, and the porosity between 12.5 and 37%. On the other hand, almost all the previous impact experiments made for ice-silicate mixture targets were conducted using the samples with the porosity less than 10% and the silicate contents varying until 50 wt %. Therefore it is necessary to study the

[1] Graduate School of Science and Technology, Kobe University, Kobe, Japan.
[2] Graduate School of Environmental Studies, Nagoya University, Nagoya, Japan.

0148-0227/08/2007JE002926$09.00

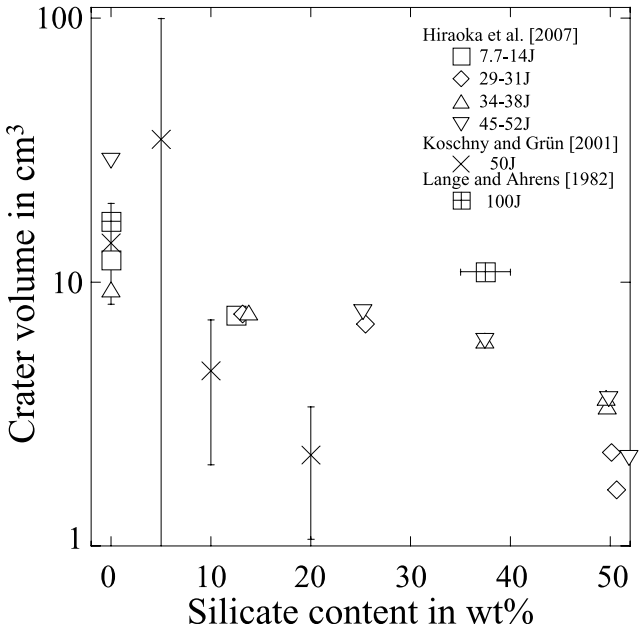

Figure 1. Relation between the silicate content and the crater volume. The symbols of *Hiraoka et al.* [2007] show the results of each kinetic energy range of impact. The plots of *Koschny and Grün* [2001] and *Lange and Ahrens* [1982] show the crater volume calculated by fitting curves of each paper at each kinetic energy.

mechanical strength of ice-silicate mixtures with wide range of silicate content and small porosities.

[5] The morphology of laboratory craters on brittle targets is typically a pit halo structure, which is similar to Rahe crater on Wild 2 [*Brownlee et al.*, 2004]. In brittle targets a compressive wave caused by an impact makes shear fracture in the target, and this region may correspond to a central pit. The compressive wave reflects as a tensile wave at the target surface. The tensile wave detaches thin fragments from the surface region, and it is called ''spallation'' [*Melosh*, 1984], which makes a halo. Thus the crater morphology and dimension of brittle targets are expected to depend on shear and tensile strength.

[6] In this study we measured the uniaxial compressive and tensile strength of the targets used by *Hiraoka et al.* [2007] at a strain rate $\sim 2 \times 10^{-3}$ s^{-1} and a temperature of 263 K, which was the same temperature with our previous study. Then the shear strength of the target was calculated from the measured values. We first present brief summary of our previous cratering experiments. Then, we describe the measurements procedure of strength and the results. In the end, we examine the relation between crater dimensions and the three kinds of strengths.

2. Brief Summary of Our Previous Study

[7] Our previous impact cratering experiments were conducted by a gas gun and a two-stage light-gas gun in a cold room (263 K) at the Institute of Low-Temperature, Hokkaido University, Japan. Cylindrical projectiles (pure ice, 15 mm in diameter, 10 mm in height and 1.6 g in weight) were used for the gas gun and truncated cone-shaped projectiles (nylon, 1.6 and 2 mm in diameter, 2.5 mm in height and 7 mg in weight) for the two-stage light-gas gun. The range of the impact velocity was from 299 to 657 m s^{-1} and from 1480 to 3684 m s^{-1}, respectively. Cylindrical targets were used for the experiments. Target size was tuned corresponding to the accelerator: 20 or 30 cm in diameter and 5 or 10 cm in height for the gas gun and 10 cm in diameter and 5 cm in height for the two-stage light-gas gun. The silicate content of the target was changed from 0 to 50 wt %. Powders of serpentine were used as the silicate content. In order to mix ice and silicate powder homogeneously in the target, we made the targets in the following procedure at 263 K. First, we broke a commercial ice block into small powders (snow) by an electric mixer. The diameter of our snow particles were in the order of 100 μm. Second, we mixed the snow into the silicate powders. These mixed powders were put into the target container, and then pushed with small quantity of purified water. We did the last process over again until all prepared water was used. The ratio of snow to water was 6:4 or 7:3. The target of 0 wt % silicate content was made by the same procedure. Cross section of the sample targets were inspected with a microscope and found to be a homogeneous mixture with some air bubble inclusions [see *Hiraoka et al.*, 2007, Figure 1]. The porosity of the target used by *Koschny and Grün* [2001] was assumed to be zero, but those of our target are estimated to be at several percent. The mean diameter of the serpentine powder was several microns in most of the experiments. The porosity of the targets was estimated to be about 10%. The crater volume was calculated by dividing the excavated mass by the target density. The excavated mass was calculated by subtracting the postimpacted target weight from the preimpacted target weight.

[8] The results showed a difference of crater morphologies between the pure ice and the ice-silicate mixture targets. Although the impact produced many cracks around the craters for the pure ice targets, there were less distinguished cracks for the ice-silicate mixture targets. The lack of spallation was also observed for the targets with higher silicate content, especially for the 50 wt % targets. The crater volume decreases with increasing silicate content. This tendency was especially clear for the results of the two-stage light-gas gun. The relation between the crater volume and the silicate content is shown in Figure 1 with the results of the other previous studies. The crater volume in the 50 wt % targets is especially smaller than those of the other targets. More detail information about our previous experiments is described by *Hiraoka et al.* [2007].

3. Measurements of Uniaxial Compressive and Tensile Strength

[9] We measured the target uniaxial compressive and tensile strength at a strain rate ($\sim 2 \times 10^{-3}$ s^{-1}) by uniaxial compression and Brazilian test [*Mellor and Hawks*, 1971] in the cold room (263 K) in the Institute of Low-Temperature, Hokkaido University. Note that the results here might be quite different at the temperatures of comets and satellites of the outer solar system. In the uniaxial compressive test, cylindrical specimens were loaded uniaxially without confining pressure and the specimen fractured with vertical cracks, which is one of the typical fracture morphology of

Table 1. Sample Dimensions and Results

Run	Sample Type[a]	Silicate Content, wt %	Sample Height, mm	σ_C or σ_T, MPa
		Uniaxial Compression Test		
S08-002	pure ice	0	46.1	3.58
S08-007	pure ice	0	48	4.98
S08-012	pure ice	0	48.6	5.13
S10-002	pure ice	0	48	5.60
S10-003	pure ice	0	49.8	6.09
S10-004	pure ice	0	48.6	5.98
S10-008	FS	5.3	47.2	6.64
S10-009	FS	5.4	46.4	7.34
S10-010	FS	5.4	46	5.97
S08-003	FS	13.4	43.9	7.69
S08-008	FS	13.3	44	7.27
S08-013	FS	12.5	47	6.15
S08-004	FS	26.4	43.9	7.90
S08-009	FS	25.6	45.2	7.65
S08-014	FS	25.4	37.5	7.36
S08-005	FS	38.5	43.8	5.32
S08-010	FS	35.6	45.1	6.92
S08-015	FS	39.1	42.8	6.87
S10-011	FS	39.3	47.2	7.01
S10-012	FS	38.3	46.9	7.66
S08-006	FS	47.9	46.5	8.26
S08-011	FS	51.3	42	8.32
S08-016	FS	50.6	43.2	9.07
S10-005	CS	49.2	47.7	8.37
S10-006	CS	50.2	49.8	8.28
S10-007	CS	50.2	48	8.04
S10-013	CD	51.3	47	8.57
S10-014	CD	51.3	45.4	8.91
S10-015	CD	51.6	47.3	8.85
		Brazilian Test		
S09-002	pure ice	0	22.3	0.70
S09-007	pure ice	0	23.8	0.74
S09-012	pure ice	0	23.1	0.772
S09-003	FS	12.6	27.5	0.567
S09-008	FS	11.4	30.2	1.07
S09-013	FS	12.0	28.6	0.868
S09-004	FS	22.9	27	0.902
S09-009	FS	23.9	22	1.25
S09-014	FS	24.7	26.9	1.40
S09-005	FS	34.9	27.1	1.63
S09-010	FS	37.2	26.1	1.93
S09-015	FS	37.1	24.9	2.01
S09-006	FS	44.9	28	1.76
S09-011	FS	48.4	26.9	2.43
S09-016	FS	47.2	28	2.35
S10-016	CS	50	26.8	[b]
S10-017	CS	50	28.8	[b]
S10-018	CS	50	15	[b]
S10-019	CD	45.5	34.3	1.32
S10-020	CD	51.2	27.7	1.52
S10-021	CD	46.6	32.4	1.37

[a]FS, CS, and CD mean the sample made by silicate powders of fine serpentine, coarse serpentine, and coarse dunite, respectively.
[b]We could not measure the strength.

brittle materials in the uniaxial compression test. The Brazilian test is one that compresses disc-shaped specimen diametrically inducing a stress that causes the sample to yield in tension. The tensile strength, σ_T is calculated using

$$\sigma_T = \frac{2F}{\pi \cdot d \cdot l}, \tag{1}$$

where F is the maximum compressive load during the measurement, d is the diameter of the sample, and l is the thickness (height) of the test specimen, respectively. On the basis of the concept postulated by Griffith, the diameter of the maximum stress circle through σ_T point on Mohr's diagram is equal to $4\sigma_T$. Consequently, the Mohr's envelope is expressed in a common tangent of the $4\sigma_T$ stress circle and a σ_C stress circle, which represents the uniaxial compressive strength. In this case, the shear strength, σ_S is approximately obtained from an intersection of τ axis in the diagram and the common tangent, and can be calculated by the following equation [*Kobayashi and Okumura*, 1971]. If $\sigma_C > 3\sigma_T$,

$$\sigma_S = \frac{\sigma_C \cdot \sigma_T}{2\sqrt{\sigma_T(\sigma_C - 3\sigma_T)}}. \tag{2}$$

[10] Ice-silicate mixture samples were prepared in cylindrical sample containers by following the same steps of the procedure in our previous experiments [*Hiraoka et al.*, 2007]. The porosity of the samples was estimated to be about 10%, which was similar to the porosity of the targets used by *Hiraoka et al.* [2007]. The silicate content of most of the samples was serpentine powders with typical diameter of several microns, similar to the powders used in the cratering experiments. We used two other kinds of powders for comparison that were coarse serpentine and dunite powders. These powders were about 200–500 μm in diameter. The silicate content of the samples using fine serpentine powder was changed from 0 to 50 wt % for both measurements. Crystalline density of serpentine and dunite is about 2.62 and 3.24 g cm^{-3}. Only 50 wt % silicate content specimens were prepared for the coarse powder samples.

[11] The test specimens were 32 mm in diameter and 43–48 mm in height for the uniaxial compression test and 20–35 mm in height for Brazilian test, respectively. Loading rate was 5 and 3 mm min^{-1} for the uniaxial compressive and Brazilian test, respectively. Thus the strain rate of the uniaxial compressive test was 1.7 to 2.2 $\times$ 10^{-3} s^{-1}. On the other hand, since the loading direction is perpendicular to the strain direction in the Brazilian test, it is not straightforward to calculate actual strain rate of Brazilian test. However, the strain rate should be close to the value of sample diameter/loading rate, 1.5 $\times$ 10^{-3} s^{-1}. The sample type and results are listed in Table 1.

4. Results

[12] Since ductile deformation was observed for ice and ice-silicate mixtures, the uniaxial compressive and tensile strength were defined by the maximum values of the stress of each stress-strain curve when we observed large cracks. For the uniaxial compressive test the stress of ice decreased rapidly after the maximum stress, and that of ice-silicate mixtures also decreased but the stress only gradually changed. In the Brazilian test the amount of plastic deformation of ice-silicate mixture samples increased with increasing silicate content. Since the contact between loading head and the sample changed from linear to planar with increasing amount of plastic deformation, the tensile strength of the specimens with the higher silicate content might not be measured precisely. However, the error due to the planar contact is probably smaller than several percent

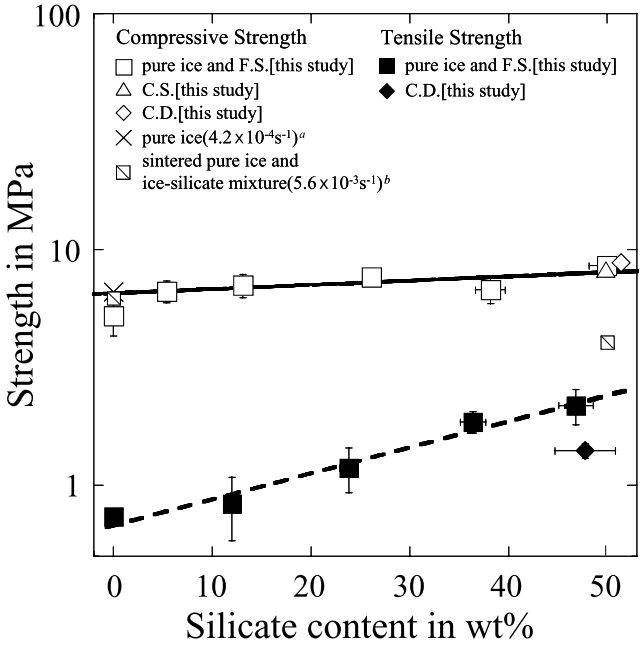

Figure 2. Relation between the silicate content and the uniaxial compressive and tensile strength. Symbols represent the sample type, which is the same in Table 1. Solid line shows the exponential fitting line of the uniaxial compressive strength for the mixture samples made by fine serpentine powders (equation (3)). Dashed line shows the exponential fitting line of the tensile strength for pure ice and the mixture samples made by fine serpentine powders (equation (4)). The superscript italic a and b denote the results of *Arakawa and Maeno* [1997] and *Arakawa and*

according to an error estimate for an arch-like contact [*Mellor and Hawks*, 1971], then within the scatter of our measurements. The results of the uniaxial compression and Brazilian test are shown in Figure 2 with the results of the previous measurements. Both strengths increase with silicate content. Figure 3 shows the samples after the uniaxial compression and Brazilian test.

[13] The uniaxial compressive strength did not differ among the samples of fine, coarse serpentine, and dunite particles. It gradually increased as the silicate content increased, with perhaps a more rapid rise between 0 and 5 wt %. The uniaxial compressive strength of the specimen with 37.5 wt % silicate content was lower than expected. The reason of this inconsistency is not clear. An empirical equation of the uniaxial compressive strength for the mixture samples made by fine serpentine powders is

$$\sigma_C = (6.5 \pm 0.5)e^{(0.004\pm0.002)R}, \quad (3)$$

where R is the silicate content and the correlation coefficient of this fitting is 0.71. *Arakawa and Maeno* [1997] measured the uniaxial compressive strength of pure ice at 263 K, which was 6.6 MPa at lower strain rate (4.2×10^{-4} s^{-1}). This pure ice sample was bubble free, which would explain why its uniaxial compressive strength was higher than those of our samples. *Arakawa and Tomizuka* [2004] measured the uniaxial compressive strength of sintered ice and ice-silicate mixtures at 263 K at 5.6×10^{-3} s^{-1}. Although their silicate content and one of the porosity were almost the same with our samples, the uniaxial compressive strength of the sintered ice-silicate mixture, whose porosity was 12.5%, was smaller than that of the sintered pure ice and our results. This maybe indicates that the cohesion between ice and silicate of our samples is stronger than that of the sintered ice-silicate mixtures of *Arakawa and Tomizuka* [2004].

[14] Although the sample height/diameter ratio (l/d) was different among the samples (from 1.2 to 1.6), the effect of this variation was small compared with the scatter caused by the individual difference among the samples as shown in the following. It is well known for the uniaxial compressive test that the uniaxial compressive strength of brittle materials is affected by the strain rate and l/d. Because the variation of the strain rate due to the difference of the sample height is very small, it would not have any significant effect on the uniaxial compressive strength. *Hawks and Mellor* [1970] showed that uniaxial compressive strength of rocks decreased up to 30% with increasing value of l/d between 1 and 2.5 or 3.0. However, our measurement results do not show this trend. This indicates that the effect of the difference of l/d is within the scatter of our measurements due to the other origins, such as the difference in the internal structure of the samples due to the preparation process.

[15] The tensile strength increased with silicate content differently from the uniaxial compressive strength. Thus the ratio between the uniaxial compressive and tensile strength changes with silicate content. Tensile strength of the specimen with dunite coarse powders 50 wt % was smaller than that of the serpentine fine 50 wt %, while the coarse serpentine 50 wt % continued plastic deformation without fracture. We could not determine the tensile strength of the coarse serpentine sample. An empirical relationship of the tensile strength for the samples made by fine serpentine powders is as follows:

$$\sigma_T = (0.68 \pm 0.07)e^{(0.026\pm0.003)R}, \quad (4)$$

where the correlation coefficient of this fitting is 0.99.

[16] Tensile strength is controlled by growth of cracks in the sample. Since silicate powders block off crack growth in the sample, the increase of the tensile strength is enhanced. This is consistent with the less number of cracks observed around the crater on ice-silicate mixture targets. The lack of spallation for the higher silicate content targets is also consistent with the increase of the tensile strength with silicate content. The difference of the tensile strength among different sample types, i.e., with serpentine and dunite, may be caused by the different volume of the silicate grains and/or different grain shapes. Since the grain density of dunite is larger than that of serpentine, total volume of the serpentine powders is larger than that of the dunite powders even if the specimens have the same silicate content in weight. Furthermore, serpentine grains have needle like structures which correspond to larger cross sections. Thus the serpen-

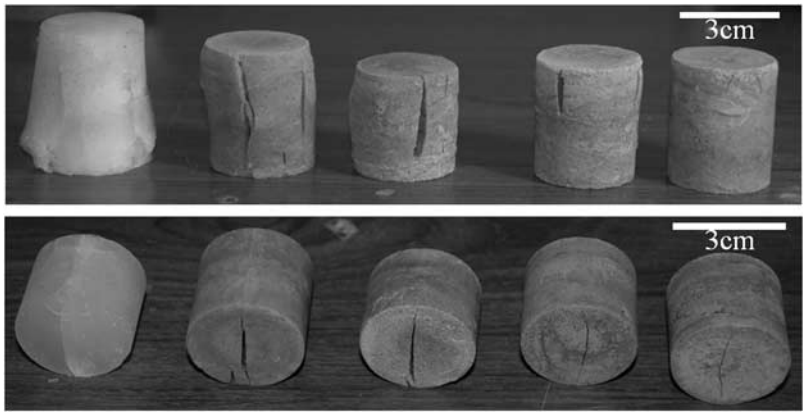

Figure 3. Samples after (top) the uniaxial compression and (bottom) Brazilian test. From the left, silicate content is 0, 12.5, 25, 37.5, and 50 wt %, respectively.

tine powders have an advantage in prevention of crack growth.

5. Relation Between Crater Dimension and Target Strength

[17] Crater volume V in the strength regime depends on impact velocity U, projectile radius a, projectile mass density δ, target strength Y, and target mass density ρ. Dimensional analysis is the primary tool used to derive scaling relationships. In the case of the strength regime, there are six parameters, with three independent dimensions of mass, length, and time. Therefore there is a simpler relation among three dimensionless combinations. In the work by *Holsapple* [1993], the choices of these groups are as follows:

$$\frac{\rho V}{m} = f\left[\frac{Y}{\rho U^2}, \frac{\rho}{\delta}\right], \tag{5}$$

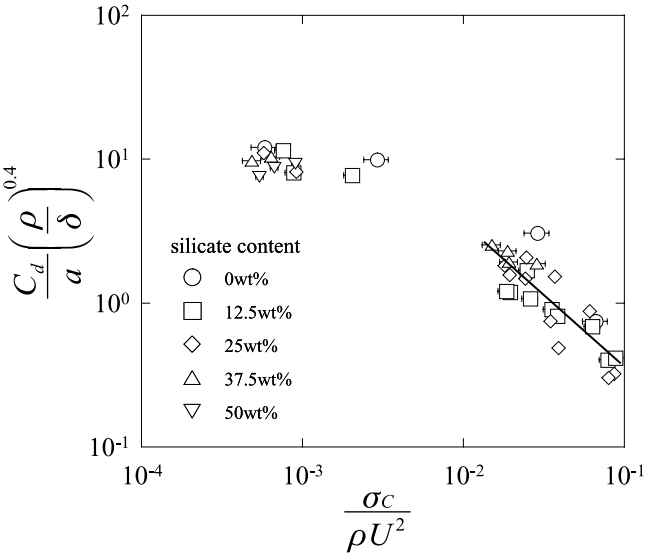

Figure 4. Relation between the dimensionless uniaxial compressive strength and the crater depth normalized by the projectile radius. The solid line shows the fitting line of the

where m is projectile mass. The left term can be changed into dimensionless crater depth or diameter. In this chapter, we discuss the most appropriate strength among the uniaxial compressive, tensile and shear strength of the target, for the dimensionless crater depth, diameter and volume, respectively. Since the density ratio of the projectile and the target in this study was changed only over factor 1.7, it is difficult to discuss and determine the dependence on the density ratio. Thus the index of the density ratio is fixed to -0.4 [*Holsapple and Housen*, 2007].

5.1. Crater Depth

[18] Figure 4 shows the relation between the dimensionless uniaxial compressive strength and the crater depth normalized by the projectile radius. The crater depth increases with the impact when it was below 700 m s^{-1}. On the other hand, the results obtained with the impact velocity between 1.5 and 3.6 km s^{-1} are almost constant. This feature can be also seen in impact experiments with rock and metal targets [*Kadono and Fujiwara*, 2005]. The crater depth is well scaled by the uniaxial compressive strength, especially for lower impact velocity. Table 2 shows correlation coefficients of fitting curves when the uniaxial compressive, tensile or shear strength are used for the scaling. A least squares fit of all results at lower impact velocity in Figure 4 gives

$$\frac{C_d}{a} = 10^{-1.4\pm0.2}\left(\frac{\sigma_C}{\rho U^2}\right)^{-1.0\pm0.1}\left(\frac{\rho}{\delta}\right)^{-0.4}, \tag{6}$$

where C_d and a are the crater depth and the projectile radius, respectively.

Table 2. Correlation Coefficients of Fitting Curves When the Uniaxial Compressive, Tensile, or Shear Strength Are Used for the Scaling

	Crater Depth/ Projectile Radius[a]	Crater Diameter/ Projectile Radius	Crater Volume/ (Projectile Radius)^3
Uniaxial compressive strength	0.74	0.91	0.73
Tensile strength	0.43	0.93	0.82
Shear strength	0.36	0.93	0.81

[a]Impact velocity ranged below 700 m s^{-1}.

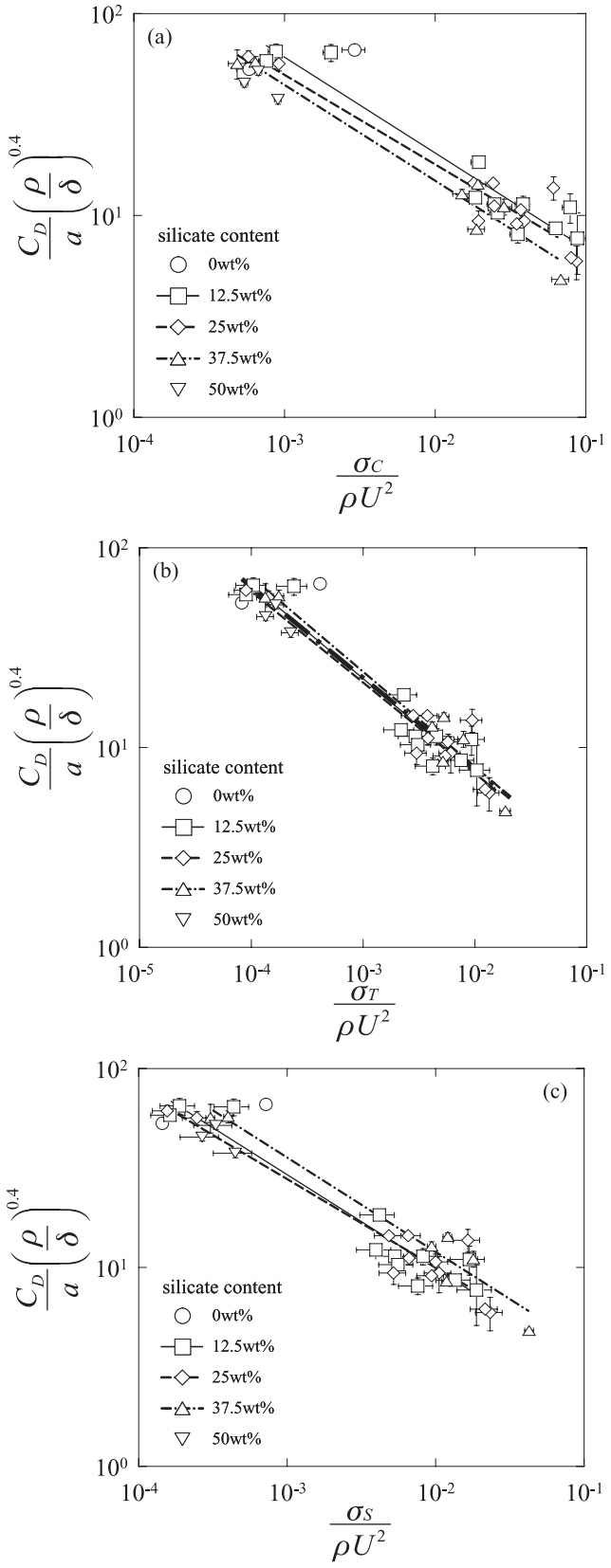

Figure 5. Relation between the (a) dimensionless uniaxial compressive, (b) tensile and shear strength, and (c) crater diameter normalized by the projectile radius. The fitting lines for the results of 12.5, 25, and 37.5 wt % silicate content are shown in plot. The bold dash-dotted line in

5.2. Crater Diameter

[19] Figures 5a, 5b, and 5c show the relation between the dimensionless uniaxial compressive, tensile and shear strength, and the crater spall diameter normalized by the projectile radius. When the normalized crater diameter is scaled by the uniaxial compressive strength, the crater diameter of the higher silicate content is still smaller than that of the lower silicate content (see Figure 5a). In the case of the normalized crater diameter scaled by the shear strength, the fitting lines in Figure 5c are still scattered. On the other hand, the tensile strength scales the crater diameter to compensate the difference of the silicate content (see Figure 5b). This is consistent with the model that the crater diameter is determined by the spallation. However, the correlation coefficients of the fitting curves shown in Table 2 are almost the same. A least squares fit of all results in Figure 5b gives

$$\frac{C_D}{a} = 10^{-0.02\pm0.07}\left(\frac{\sigma_T}{\rho U^2}\right)^{-0.46\pm0.02}\left(\frac{\rho}{\delta}\right)^{-0.4}, \qquad (7)$$

where C_D is the crater diameter.

5.3. Crater Volume

[20] Figures 6a, 6b, and 6c shows the relation between the dimensionless uniaxial compressive, tensile and shear strength, and the normalized crater volume. The normalized crater volume is better scaled by the tensile strength to compensate the difference of the silicate content than by the uniaxial compressive strength or the shear strength (see Figures 6a, 6b, and 6c). However, the correlation coefficients of the fitting curves shown in Table 2 are almost the same similar to the crater diameter. A least squares fit of all results in Figure 6b gives

$$\frac{V}{a} = 10^{-1.4\pm0.2}\left(\frac{\sigma_T}{\rho U^2}\right)^{-1.15\pm0.07}\left(\frac{\rho}{\delta}\right)^{-0.4}. \qquad (8)$$

[21] The reason why the crater volume is controlled by the tensile strength is as follows. The tensile strength increases with the silicate content more rapidly than the uniaxial compressive strength. Furthermore, the crater volume is roughly in proportion to the crater depth and square to the crater diameter. Thus the crater volume is controlled by the tensile strength. Increase of the tensile strength with silicate content is probably the main reason why the crater volume decreases with silicate content.

6. Summary

[22] Previous impact cratering experiments indicate that the crater volume in ice-silicate mixture targets decreases with increasing silicate content. In order to understand this tendency we measured the uniaxial compressive and the tensile strength of ice-silicate mixtures with silicate content at a low strain rate ($\sim 2 \times 10^{-3}$ s^{-1}) and calculated the shear strength. Both the uniaxial compressive and tensile strengths increased with silicate content, although the gradient of increase was different. The uniaxial compressive strength gradually increased as the silicate content increased, with perhaps a more rapid rise between 0 and 5

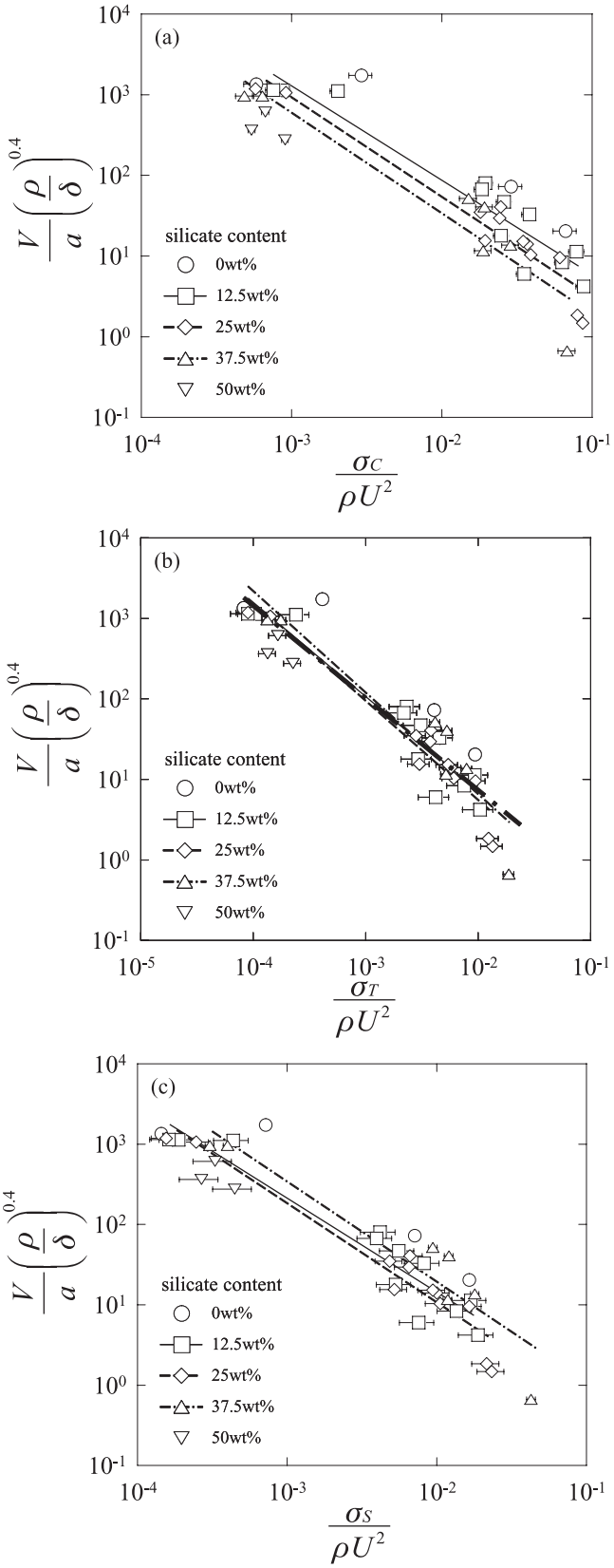

Figure 6. Relation between (a) the dimensionless uniaxial compressive, (b) tensile and shear strength, and (c) normalized crater volume. The fitting lines for the results of 12.5, 25, and 37.5 wt % silicate content are shown in plot. The bold dash-dotted line in Figure 6b shows the wt %. When we apply these strengths to the previous results on laboratory impact cratering experiments [*Hiraoka et al.*, 2007], the crater depth with the impact velocity ranged below 700 m s^{-1} is well scaled by the uniaxial compressive strength of the target. The crater diameter and the crater volume are scaled by the target tensile strength by compensating the difference of the silicate content. Increase of the tensile strength with silicate content is probably the main reason why the crater volume decreases with silicate content.

[23] **Acknowledgments.** We thank K. Holsapple of University Washington and P. Michel of Observatoire de la Cote d'Azur for discussing the cratering mechanism and the strength of brittle materials. We also thank T. Yamamoto and A. Kouchi of Institute of Low Temperature Science, Hokkaido University, for considerable support during the measurements and K. Sangen of Kobe University for his preparation of the sample containers. This work was supported by the cooperative research of Institute of Low Temperature Science, Hokkaido University and the "21st Century COE Program of Origin and Evolution of Planetary Science" of the Ministry of Education, Culture, Sports, Science and Technology (MEXT), Japan.

References

Arakawa, M., and N. Maeno (1997), Mechanical strength of ice under uniaxial compression, *Cold Regions Sci. Technol.*, *26*, 215–229.

Arakawa, M., and D. Tomizuka (2004), Ice-silicate fractionation among icy bodies due to the difference of impact strength between ice and ice-silicate mixture, *Icarus*, *170*, 193–201.

Brownlee, D. E., et al. (2004), Surface of young Jupiter Family Comet 81 P/Wild 2: View from the Stardust spacecraft, *Science*, *304*, 1764–1769.

Estrada, P. R., and J. N. Cuzzi (1996), Voyager observations of the color of Saturn's rings, *Icarus*, *122*, 251–272.

Hawks, I., and M. Mellor (1970), Uniaxial testing in rock mechanics laboratories, *Eng. Geol.*, *4*, 177–285.

Hiraoka, K., M. Arakawa, K. Yoshikawa, and A. M. Nakamura (2007), Laboratory experiments of crater formation on ice-silicate mixture targets, *Adv. Space Res.*, *39*, 392–399.

Holsapple, K. A. (1993), The scaling of impact processes in planetary sciences, *Annu. Rev. Earth Planet Sci.*, *21*, 333–373.

Holsapple, K. A., and K. R. Housen (2007), A crater and its ejecta: An interpretation of Deep Impact, *Icarus*, *187*, 345–356.

Kadono, T., and A. Fujiwara (2005), Cavity and crater depth in hypervelocity impact, *Int. J. Impact Eng.*, *31*, 1309–1317.

Kato, M., Y. Iijima, M. Arakawa, Y. Okimura, A. Fujimaru, N. Maeno, and H. Mizutani (1995), Ice-on-ice impact experiments, *Icarus*, *133*, 423–441.

Keller, H. U., et al. (2005), Deep Impact observations by OSIRIS onboard the Rosetta spacecraft, *Science*, *310*, 281–283.

Kempf, S., et al. (2005), Composition of Saturnian stream particles, *Science*, *307*, 1274–1276.

Kobayashi, R., and K. Okumura (1971), Study on shear strength of rocks, *J. Min. Inst. Jpn.*, *87*(999), 407–412.

Koschny, D., and E. Grün (2001), Impact into ice-silicate mixtures: Crater morphologies, volumes, depth-to-diameter ratios, and yield, *Icarus*, *154*, 391–401.

Lange, M. A., and T. J. Ahrens (1982), Impact cratering in ice- and ice-silicate targets: An experimental assessment, *Lunar Planet. Sci.*, *XIII*, 415–416.

Mellor, M., and I. Hawks (1971), Measurement of tensile strength by diametral compression of discs and annuli, *Eng. Geol.*, *5*, 173–225.

Melosh, H. J. (1984), Impact ejection, spallation, and the origin of meteorites, *Icarus*, *59*, 234–260.

Porco, C. C., et al. (2005), Cassini imaging science: Initial results on Phoebe and Iapetus, *Science*, *307*, 1237–1242.

M. Arakawa, Graduate School of Environmental Studies, Nagoya University, Furou-cho, Chikusa, Nagoya, Aichi, 464-8601, Japan.

K. Hiraoka A. M. Nakamura, and M. Setoh, Graduate School of Science and Technology, Kobe University, 1-1 Rokkodai-cho, Nada-ku, Kobe, 657-8501, Japan. (kensuke@kobe-u.ac.jp)